Talanta 85 (2011) 325–332

Contents lists available at ScienceDirect

Talanta

journal homepage: www.elsevier.com/locate/talanta

The maintenance of the second-order advantage: Second-order calibration of excitation–emission matrix fluorescence for quantitative analysis of herbicide napropamide in various environmental samples

Yuan-Na Li, Hai-Long Wu*, Xiang-Dong Qing, Chong-Chong Nie, Shu-Fang Li, Yong-Jie Yu, Shu-Rong Zhang, Ru-Qin Yu

State Key Laboratory of Chemo/Biosensing and Chemometrics, College of Chemistry and Chemical Engineering, Hunan University, Changsha 410082, PR China

ARTICLE INFO

Article history:
Received 18 December 2010
Received in revised form 23 March 2011
Accepted 25 March 2011
Available online 5 April 2011

Keywords:
Second-order calibration
Napropamide
APTLD
Excitation–emission matrix fluorescence
Calibration maintenance

ABSTRACT

A rapid non-separative spectrofluorometric method based on the second-order calibration of excitation–emission matrix (EEM) fluorescence was proposed for the determination of napropamide (NAP) in soil, river sediment, and wastewater as well as river water samples. With 0.10 mol L^{-1} sodium citrate–hydrochloric acid (HCl) buffer solution of pH 2.2, the system of NAP has a large increase in fluorescence intensity. To handle the intrinsic fluorescence interferences of environmental samples, the alternating penalty trilinear decomposition (APTLD) algorithm as an efficient second-order calibration method was employed. Satisfactory results have been achieved for NAP in complex environmental samples. The limit of detection obtained for NAP in soil, river sediment, wastewater and river water samples were 0.80, 0.24, 0.12, 0.071 ng mL^{-1}, respectively. Furthermore, in order to fully investigate the performance of second-order calibration method, we test the second-order calibration method using different calibration approaches including the single matrix model, the intra-day various matrices model and the global model based on the APTLD algorithm with nature environmental datasets. The results showed the second-order calibration methods also enable one or more analyte(s) of interest to be determined simultaneously in the samples with various types of matrices. The maintenance of second-order advantage has been demonstrated in simultaneous determinations of the analyte of interests in the environmental samples of various matrices.

1. Introduction

With the development of modern second-order instruments which generate a lot of second-order data, second-order calibration methods are gaining widespread acceptance by the analytical community. Second-order calibration method allows concentrations and spectral profiles of the sample components to be extracted in the presence of any number of unexpected constituents [1–4]. This property, named the "second-order advantage", is especially convenient when analysts handle complex matrices. In recent decades, a great variety of second-order calibration methods have been produced for a three-way data array, such as parallel factor analysis (PARAFAC) [5,6], generalized rank annihilation method (GRAM) [7], multivariate curve resolution-alternating least squares (MCR-ALS) [8], alternating trilinear decomposition (ATLD) [9], self-weighed alternating trilinear decomposition (SWATLD) [10] and alternating penalty trilinear decomposition (APTLD) [11]. Taking into advantage of the property, it enables several analytes of interest to be determined simultaneously in one set of matrix samples, which has been demonstrated and applied in many analytical fields [12–16], e.g. pharmaceuticals, biological matrices, foods, environmental matrices and synthetic samples. On the other hand, it also enables one or more analyte(s) of interest to be determined simultaneously in samples with various types of matrices, there are a few applications in this aspect. For example, testosterone propionate was determined in several cosmetics using excitation–emission matrix fluorescence with the aid of second-order calibration methods [17].

The maintenance of second-order advantage from day to day or in various different matrices is an interesting problem when an analytical method is proposed for rapid routine daily use. The PARAFAC model applied to excitation–emission matrix (EEM) fluorescence signals and through the global models strategy has been proved useful to predict accurately samples measured on different days, by different analysts and even in the presence of non-modeled interferents by Giméneza et al. [18]. In addition, the prediction quality of second-order calibration as a function of the size of the calibration set, the number and degree of overlap of new interferents and

* Corresponding author. Tel.: +86 731 88821818; fax: +86 731 88821818.
E-mail address: hlwu@hnu.cn (H.-L. Wu).

0039-9140/$ – see front matter © 2011 Elsevier B.V. All rights reserved.
doi:10.1016/j.talanta.2011.03.067

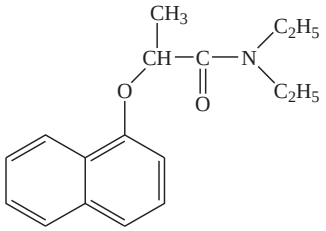

Fig. 1. Structure of napropamide (NAP).

the type and magnitude of noise was investigated by Rinnan [19], and the guidelines were given on how to implement predictions in PARAFAC-based second-order calibration. However, there has not been much work on the comparison of prediction quality for the single matrix model (the calibration set combined with one-matrix samples), the intra-day various matrices model (the calibration set combined with environmental samples of different matrices on the same day) and the global (inter-day various matrices) model (two calibration sets combined with environmental samples of different matrices on different days). The maintenance of the second-order advantage has not been fully demonstrated one or more analyte(s) of interest are determined in samples with various types of matrices.

Herbicides are chemicals that often employed to kill weeds without causing injury to desirable vegetation. Napropamide [N,N-diethyl-2-(1-naphthalenyloxy) propanamide], is a highly effective broad-spectrum amide herbicide and widely used as pre-emergence herbicide weeding out most annual monocotyledon and broadleaf weeds in many agricultural cultivations, such as tea, ground nut, citrus, tobacco, and tomatoes [20]. However, the toxicity of this herbicide has been studied, which showed that inhalation, contact with eyes, skin and clothing and prolonged and repeated exposure must be avoided [21]. Furthermore, due to its long half-life (approximate 70 days), the residue of napropamide in soils may affect the growth of succeeding crops. Besides, its property of moderate adsorption/desorption on soils also makes napropamide fairly mobile and leaching, thus resulting in contamination of wastewater, rivers and river sediments [22]. Therefore, its high use on agrarian activity resulted in increasing need for sensitive analytical methods for napropamide determination in different matrices, such as soil, wastewater, river water, and river sediments.

Owing to its intrinsic sensitivity, ease of use, and availability of instruments, fluorescence spectroscopy provides a valuable tool to analytical chemists. Nevertheless, fluorescence signal peak of substance is usually broad, so in complex mixtures the signal will be overlapped. Moreover, when a given sample carries unexpected fluorescent constituents that have not been modeled during the calibration phase, a convenient way of quantifying analytes of interest in complex mixtures is by resorting to higher-order data coupled to the second-order advantage. The structure of napropamide (Fig. 1) has a naphthalene ring, which connects with a conjugate double bond system; it can give off strong fluorescence in proper conditions [23]. So, in this paper, we have attempted to make use of excitation–emission matrix (EEM) fluorescence to estimate herbicide napropamide in various environmental samples with the aid of second-order calibration method.

In the present study, we developed a rapid and sensitive non-separative excitation–emission fluorescence method for the determination of herbicide napropamide in soil, river sediment, wastewater and river water samples using the APTLD algorithm as a second-order calibration method. The figures of merit involving the sensitivity (SEN), the selectivity (SEL) and the limit of detection (LOD), as well as the limit of quantification (LOQ) were investigated. In addition, a comparison of prediction qualities among the single matrix model, the intra-day various matrices model and the global model in the APTLD algorithm-based second-order calibration has been done in this work.

2. Experimental

2.1. Reagents and chemicals

All reagents and chemicals used were of analytical reagent grade. Napropamide (NAP) (purchased from Dr. Ehrenstorfer Corporation, Germany, content > 99.5%) was used without further purification. All glass wares were previously soaked in chromate lotion overnight, and then rinsed with ultrapure-grade water prior to the use. A stock solution of 50.0 μg mL^{-1} was prepared by accurately weighing the required amounts of NAP and dissolving in acetonitrile and diluting with ultrapure-grade water in a 100 mL brown volumetric flask, and then stored at 4 °C in a refrigerator until used. The working solutions of NAP were daily prepared by diluting the stock solutions with ultrapure-grade water. The 0.10 mol L^{-1} sodium citrate–hydrochloric acid (HCl) buffer solution of pH 2.2 was prepared.

2.2. Instrumentation and software

All of the fluorescence measurements were performed on an F-4500 fluorescent spectrophotometer (Hitachi, Japan), which was equipped with a continuous 150-W Xenon arc lamp and interfaced to a personal computer. In all cases, a 1.00 cm quartz cell was used at room temperature. In the MATLAB environment all home-made programs were written and further used for data analysis. All calculations were carried out on a microcomputer under the Windows XP operating system.

All of the spectral surfaces were recorded at excitation wavelengths varying from 250 to 310 nm in 2 nm steps, and emission wavelengths varying from 320 to 396 nm in 2 nm steps with a scanning rate of 1200 nm min^{-1}. The excitation and emission monochromator slit widths were 5.0 nm, respectively. For a single sample, a matrix of size of 39 × 31 was obtained. The used spectral ranges were selected after a suitable consideration of the spectral regions corresponding to maximum signals for the analyte and avoiding useless background signals, such as Rayleigh and Raman scattering.

2.3. Environmental sample collection and preparation

The soil samples and river sediment samples were collected from the cropland and the bank of the Xiangjiang River in Hunan Province of China, respectively. The collected samples were stored in plastic bags and dried at room temperature, and then ground with a mortar. Firstly, 100 mL of solvent (methanol:acetonitrile = 1:1, v/v) were added to 100 g soil and river sediment samples, respectively. Secondly, the mixtures were shaken vigorously for 30 min and left for a whole day for adequate extraction of NAP. Finally the mixtures were filtered and the filtrates were evaporated to dryness, and then the residues were reconstituted with ultrapure-grade water. The wastewater samples and river water samples were collected from a pool in residential area and the Xiangjiang River in Changsha, China, respectively. Both water samples were filtered through filter paper to remove suspended sediments and solid materials. The filtrates were stored at 4 °C in the refrigerator before being used.

2.4. Analytical procedure

The first calibration set consisting of nine calibration samples (at concentrations 30, 50, 70, 90, 120, 140, 160, 180, 200 ng mL^{-1}) was

Table 1
Results from APTLD analysis in single matrix model of soil samples (*S*), sediment samples (*D*), wastewater samples (*W*), and river water samples (*R*), respectively.

Sample no.	Actual value of NAP (ng mL^{-1})				Recovery (%)			
	S	*D*	*W*	*R*	*S*	*D*	*W*	*R*
P1	60	100	100	80	108.7	92.1	105.5	97.9
P2	80	130	130	100	105.4	100.8	104.1	101.5
P3	100	150	150	130	99.7	97.7	102.0	100.8
P4	130	170	170	150	97.6	104.8	102.7	100.2
P5	150	–	190	170	96.8	–	101.7	90.8
P6	170	–	200	190	107.2	–	102.3	95.4
Average recovery (%)					102.6 ± 4.5	98.9 ± 4.0	103.0 ± 1.2	97.8 ± 3.1
RMSEP (ng mL^{-1})					6.72	6.89	4.89	8.93
REP (%)					5.84	5.01	3.12	6.31

The root-mean-square error of prediction (RMSEP) can be calculated in terms of the formula as RMSEP $= [1/(M-1)\sum_{m=1}^{M}(c_{act}-c_{pred})^2]^{1/2}$, where M is the number of prediction samples, c_{act} and c_{pred} are the actual and predicted concentrations of the analytes, respectively. The relative error of prediction (REP): REP = $(100 \times \text{RMSEP})/c_{ave}$, here c_{ave} is the average concentration of analyte in prediction samples.

constructed; at the same time, six soil samples and four river sediment samples were spiked with suitable amounts of standard NAP solutions. The final analyte concentrations for prediction samples were within the concentration range of the calibration samples as listed in Table 1. The spectra of ultrapure-grade water blank solution and each soil, river sediment blank solution were recorded in triplicate experiments during the whole analytical procedure. The fluorescent spectra were measured in random order according to the sample number using the experimental parameters stated under Section 2.2.

At the next day, the second calibration set of eight samples (at almost the same concentration as the first calibration set) was constructed. In addition, six prediction samples were constructed by spiking wastewater and river water with NAP to yield concentrations as shown in Table 1, respectively. The spectra of ultrapure-grade water blank solution and each wastewater, river water blank solution were recorded in triplicate experiments during the whole analytical procedure. The fluorescent spectra were measured in random order according to the sample number using the experimental parameters stated under Section 2.2.

2.5. Chemometric analysis

Suppose a given sample produces a data matrix of size $I \times J$, where I and J denote the number of data points in the first and second dimensions, respectively. In the case of excitation–emission matrix fluorescence, I is the number of emission wavelengths and J is the number of excitation wavelengths. If K samples, consisting of calibration samples and prediction samples, are stacked, a three-way data array $\underline{\mathbf{X}}$ is obtained with dimensions of $I \times J \times K$. A trilinear model for such a three-way array $\underline{\mathbf{X}}$ has the form:

$$x_{ijk} = \sum_{n=1}^{N} a_{in} b_{jn} c_{kn} + e_{ijk}, \qquad i=1,2,\ldots,I, \quad j=1,2,\ldots,J, \quad k=1,2,\ldots,K. \tag{1}$$

Here x_{ijk} is the element of $\underline{\mathbf{X}}$, a_{in}, b_{jn} and c_{kn} are the elements of the $I \times N$ matrix **A** corresponding to the emission spectral profiles, the $J \times N$ matrix **B** corresponding to the excitation spectral profiles and the $K \times N$ matrix **C** corresponding to the relative concentrations, respectively. e_{ijk} is the element of a three-way residual array $\underline{\mathbf{E}}$. N denotes the number of factors, which is really the total number of detectable physically meaningful components of interest as well as the interferents and the background.

Second-order calibration requires decomposition of a three-way data array and regression of relative concentration of the component(s) of interest in sample space against the corresponding standard concentrations. For decomposition of a three-way data array, several algorithms have been suggested.

The alternating penalty trilinear decomposition (APTLD) algorithm was developed by our group [11]. The method decomposes three-way data arrays by utilizing the alternating least-squares principle and the alternating penalty constraints to minimize three different alternating penalty errors simultaneously. The APTLD algorithm can avoid the two-factor degeneracy problem and relieve the slow convergence problem. In addition, it is insensitive to the estimated component number, thus it avoids the difficulty of determining a correct component number for the model. The APTLD theory was well documented [11], so it is not described here.

2.6. Figures of merit

With the aim of evaluating the results obtained by using the above second-order calibration algorithm, the figures of merit including the sensitivity (SEN), the selectivity (SEL), the limit of detection (LOD) and the limit of quantification (LOQ) are reckoned. In second-order calibration, they are understood in terms of the useful concept of net analyte signal (NAS), firstly developed by Lorber [24]. The sensitivity (SEN) for a particular analyte is estimated according to the net analyte signal at unit concentration [25], and the selectivity (SEL) is estimated in terms of the ratio of the sensitivity to the total signal [26]. The following equations can be obtained to estimate the SEN and the SEL in the present work:

$$\text{SEN} = k\{[(\mathbf{A}^{\mathrm{T}}\mathbf{A})^{-1}]_{nn}[(\mathbf{B}^{\mathrm{T}}\mathbf{B})^{-1}]_{nn}\}^{-1/2}, \tag{2}$$

$$\text{SEL} = \{[(\mathbf{A}^{\mathrm{T}}\mathbf{A})^{-1}]_{nn}[(\mathbf{B}^{\mathrm{T}}\mathbf{B})^{-1}]_{nn}\}^{-1/2}. \tag{3}$$

Here nn designates the (n,n) element of a matrix, k is the total signal for component n at unit concentration, in this paper, and k is also the parameter converting scores to concentrations.

The limit of detection (LOD) is calculated with the formula: LOD = 3.3 $s(0)$ [27,28], where $s(0)$ is the standard deviation in the predicted concentrations of the analyte of interest in three blank samples. The limit of quantification (LOQ) is computed according to LOQ = 10 $s(0)$.

3. Results and discussion

According to the aforementioned wavelength range selection, at the suggested optimum condition the interfering effects of Rayleigh and Raman scattering are at the lowest levels. However, in the analysis of environmental samples, such as soil, river sediment, wastewater and river water, simple pretreatment is necessary to convert soil and river sediment samples into liquid form prior to the measurement, while wastewater and river water samples are used directly except for filtering the suspended solid materials and sediments. Whereas, such simple pretreatment is usually not selective enough, and often partial interfering matrices from environmental samples are co-extracted with the component of interest. Moreover, the spectral overlapping between the NAP and ingredients

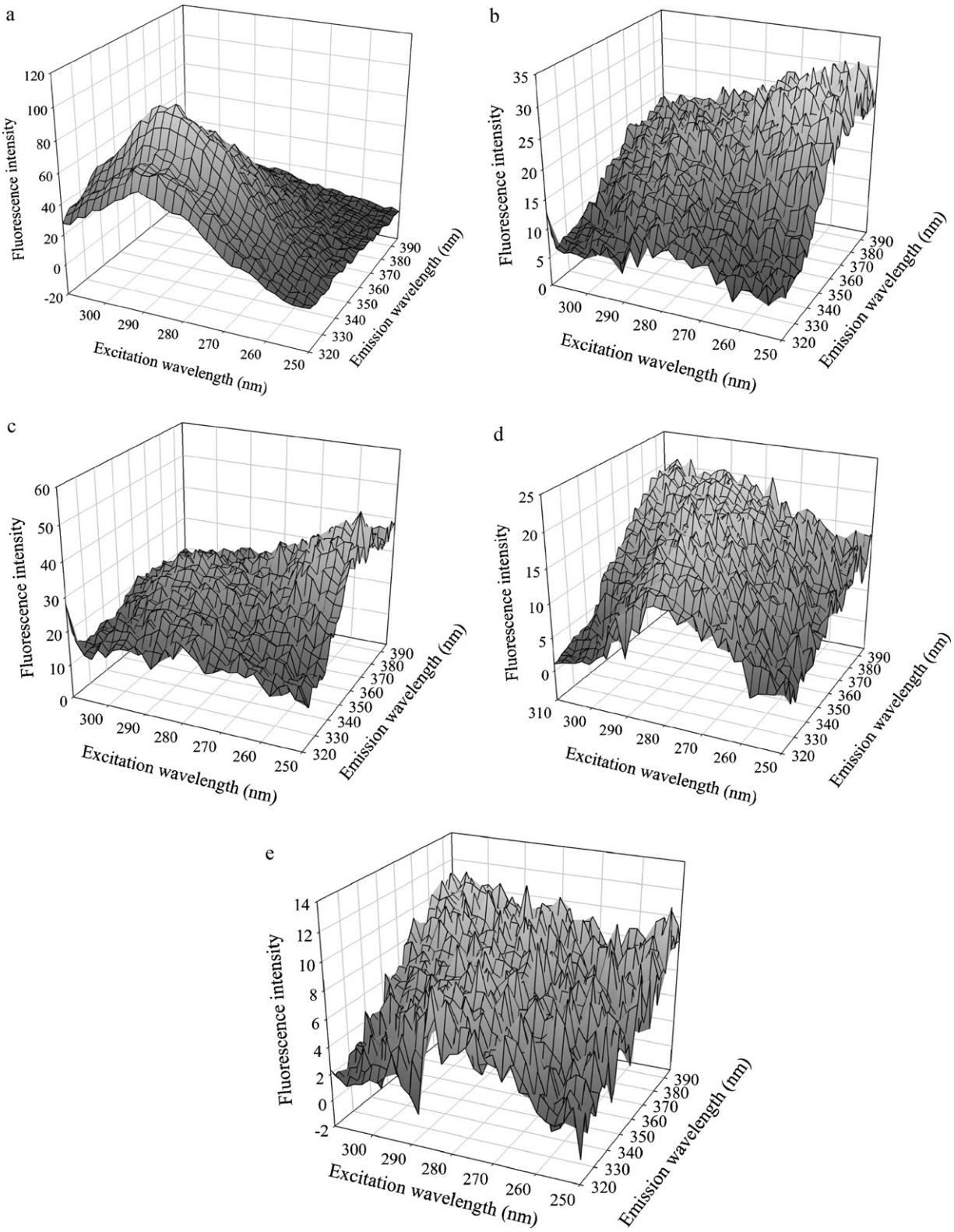

Fig. 2. The excitation–emission matrix fluorescent spectra of NAP and blank environmental samples: (a) pure NAP, (b) blank soil sample, (c) blank river sediment sample, (d) blank wastewater sample and (e) blank river water sample.

from environmental samples is very significant and hinder the direct fluorescent quantification of NAP in these matrices. The three-dimensional fluorescent spectra of pure NAP and blank environmental samples are shown in Fig. 2. As can be appreciated, heavy fluorescence overlapping between the analyte and the environmental background of the samples occurs in the chosen region, restricting the use of univariate method. Fortunately, a modern approach to overcome this problem is the advanced second-order chemometric method, which might light to a new avenue to replace the "physical or chemical separation" with "mathematical separa-

tion" strategy through separating the signals of target analyte(s) away from those of uncalibrated background or interferences. In this paper, the APTLD algorithm was recommended to assay the concentrations of NAP in soil, river sediment, wastewater and river water samples simultaneously, which fully exploit the "second-order advantage".

3.1. Single matrix model

Soil samples. The prediction set of six soil samples was combined with the first calibration set to construct a three-way data array of size $39 \times 31 \times 15$, which was then decomposed by the APTLD algorithm.

River sediment samples. For recovery analysis of river sediment samples, a size of $39 \times 31 \times 13$ data array, here the number 13 corresponds to nine calibration samples plus four river sediment samples, was obtained. Subsequently, the three-way data array will be treated with the APTLD algorithm.

Wastewater samples. A recovery study by spiking six wastewater samples of NAP was carried out. The six wastewater samples was combined with the second calibration set to construct a three-way data array of size $39 \times 31 \times 14$, which was treated with the APTLD algorithm.

River water samples. For quantification of NAP in river water samples, a prediction set of six river water samples was constructed. The calibration set and the river water samples were put together making one data array of size $39 \times 31 \times 14$, here the number 14 corresponds to eight calibration samples plus six river water samples, The three-way data array was decomposed by the APTLD algorithm.

The property of the "second-order advantage" is powerful and the second-order calibration methods can not only determine the concentration of the analyte(s), but also can extract the profiles of analyte(s) from different matrices, it has been proved that the spectral profiles of the analyte(s) in different complex matrices are almost the same [29–31]. Therefore, although three-way arrays of the soil, river sediment, wastewater and river water samples were decomposed respectively, the resolved excitation–emission spectral profiles of NAP together with the different interferences of environmental samples were plotted in one figure, i.e. Fig. 3.

Fig. 3 shows the resolved excitation–emission spectral profiles together with the actual one of NAP in different environmental samples using the APTLD algorithm. Fig. 3(a) and 3(b) shows the excitation spectral profile and the emission spectral profile, respectively. These emission and excitation spectral profiles were collected into the matrices **A** and **B**, respectively. One can observe that the spectral profile of NAP and the spectral profile of the interferences of different environmental samples were overlapped heavily. Therefore, it is difficult to determine NAP in the environmental samples in a straightforward way using sensitive spectrofluorimetry without further separation. From the figures, the resolved spectral profile of NAP and the actual one are almost the same, which implies the good ability of qualitative analysis of the second-order calibration methods. The results from the predictions for the different environmental samples are summarized in Table 1. The average recoveries of NAP were $(102.6 \pm 4.5)\%$, $(98.9 \pm 4.0)\%$, $(103.0 \pm 1.2)\%$ and $(97.8 \pm 3.1)\%$ in soil, river sediment, wastewater, and river water samples, respectively. The root-mean-square errors of prediction (RMSEP) of NAP were 6.72, 6.89, 4.89 and 8.93 ng mL^{-1} in soil, river sediment, wastewater, and river water samples, respectively. And the relative errors of prediction (REP) of NAP in soil, river sediment, wastewater and river samples were 5.8%, 5.0%, 3.1%, 6.3%, respectively.

For the sake of evaluating the performance of the proposed approaches, the figures of merit including the sensitivity (SEN), the selectivity (SEL), the limit of detection (LOD), and the limit of quantification (LOQ) for the determination of NAP in different environmental samples including soil, river sediment, wastewater, and river water samples, were investigated and summarized in Table 2. The LODs for NAP in soil, river sediment, wastewater, and river water samples were calculated to be 0.80, 0.24, 0.12, 0.071 ng mL^{-1}, respectively.

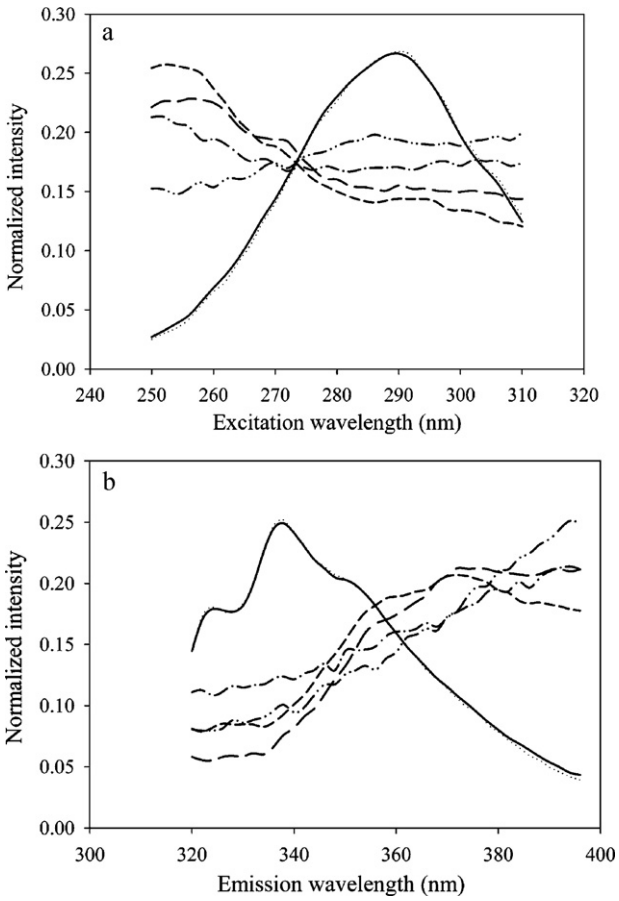

Fig. 3. Normalized excitation (a) and emission (b) profiles, which were resolved from EEM fluorescence of soil, river sediment, wastewater and river water samples by the APTLD method, respectively. Solid, long-dash, short-dash, dash-dot-dot, dash-dot lines represent the spectral profiles of NAP, interference of soil, river sediment, wastewater, river water samples, respectively. The dotted line denotes actual NAP.

One can find that the second-order calibration method based on the APTLD algorithm can yield satisfactory predictive capacity for determination of NAP in different environmental samples. However, the power of the "second-order advantage" could not be completely appreciated until its capacity to determine the analyte(s) in various nature matrices simultaneously is demonstrated. Therefore, the specific implementation as well as the study of daily various matrices model and global (inter-daily various matrices) model will be discussed in detail in the following part.

Table 2
Figures of merit for quantitative analysis of NAP in soil samples (*S*), river sediment samples (*D*), wastewater samples (*W*) and river water samples (*R*) by APTLD algorithm.

Figures of merit	*S*	*D*	*W*	*R*
RMSEP (ng mL^{-1})	6.72	6.89	4.44	7.70
SEN (mL ng^{-1})	4.80	4.65	2.91	3.40
SEL	0.39	0.38	0.23	0.27
LOD (ng mL^{-1})	0.80	0.24	0.12	0.071
LOQ (ng mL^{-1})	2.42	0.74	0.36	0.21

3.2. Intra-day various matrices model

Soil and river sediment samples. The first calibration set of nine calibration samples, six soil samples and four river sediment samples were measured in the same day. We have attempted to stack the calibration data set and two different matrix sets together to construct a new three-way data array of size $39 \times 31 \times 19$, and then the three-way data array was decomposed by the APTLD algorithm. Table 3 collects the results of NAP in intra-day various matrix samples.

Wastewater and river water samples. As the aforementioned, the second calibration set of eight samples, six wastewater samples and six river water samples were prepared in the next day. A new three-way data array of size $39 \times 31 \times 20$, here the number 20 represents eight calibration plus six wastewater samples and six river water samples, was obtained. Subsequently, the three-way data array was treated with the APTLD algorithm. The results of NAP in daily various matrices samples are listed in Table 3.

From Table 3, the average recoveries of NAP were $(101.6 \pm 4.3)\%$, $(99.3 \pm 3.9)\%$, $(103.1 \pm 1.2)\%$ and $(97.1 \pm 3.1)\%$ in soil, river sediment, wastewater, and river water samples, respectively. The root-mean-square errors of prediction (RMSEP) of NAP were 6.39, 6.88, 4.95 and 9.48 ng mL^{-1} in soil, river sediment, wastewater, and river water samples, respectively. And the relative errors of prediction (REP) of NAP in soil, river sediment, wastewater and river samples were 5.6%, 5.0%, 3.2%, 6.7%, respectively.

The results showed that there was no significant difference between the results of the intra-day various matrices model and those of the single matrix model. It was proved that the second-order calibration also enables one or more analytes of interest to be determined in various matrices simultaneously with one calibration set, which save much time for analysis.

3.3. Global (inter-daily various matrices) model

Joining the two calibration sets and four different environmental samples sets, we obtained the global model which included the variability from day to day and of different matrices. A new three-way data array of size $39 \times 31 \times 39$ was constructed. Subsequently, the three-way data array will be decomposed by the APTLD algorithm. Prior to the analysis, in order to ensure the performance of the adopted algorithms because of the complexity of the four different matrices samples, the core consistency diagnostic (CORCONDIA) test [32] was used to determine the number of components in the present work. A two-component model was constructed according to the results from the CORCONDIA test. Fig. 4 shows the core consistency values as a function of the number of components. As can be appreciated, a two-component model has a core consistency value of 100%, while a three-component model has a core consistency value less than 40%, which means that two is the appropriate number of components in the analysis. Additionally, in the analysis of environmental samples, even though the ingredients are different from matrix to each other, the extracted components from different matrices may be analogous and some of them have such highly similar fluorescent properties that the proposed approaches cannot resolve these into separated factors. Therefore, two components indicated the NAP and interference from environmental matrices, respectively.

Fig. 5 shows the actual spectral profiles and the profiles from the decomposition of the three-way data array abovementioned by using the APTLD algorithm with two factors. The profile associated with the excitation mode is shown in Fig. 5(a) and the profile related to the emission mode is shown in Fig. 5(b). The figure indicated that the spectral profiles of interference from the environmental samples spread all measured wavelength, both excitation and emission wavelengths, and overlap with NAP spectral profile. Looking at the

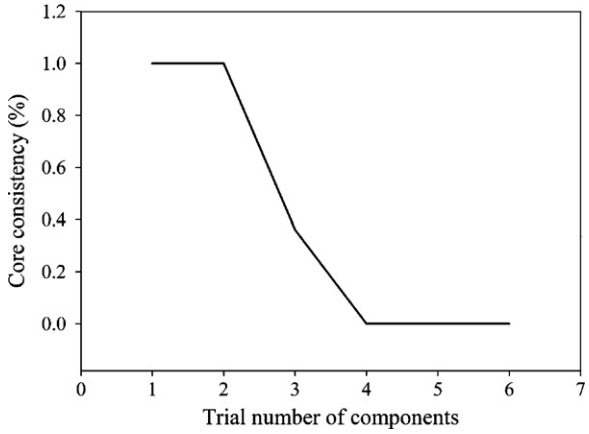

Fig. 4. Core consistency values as a function of the trial number of components for the analysis of the inter-daily various environmental matrices samples.

profiles one can judge the difficulty in analyzing the environmental samples of various matrices. Moreover, the dotted line denotes the actual spectral property of NAP. It can be observed that not only are the resolved excitation and emission spectral profiles of NAP nearly the same as the actual one, but also the structures of the excitation and emission profiles of the interesting analyte are not affected by the variety of the data array constructed model chosen, which indicated that the obtained results are accurate and reliable.

With the aid of the spectral profiles extracted, the corresponding column in the relative concentration modes to the NAP can be found to evaluate the actual concentrations of NAP in envi-

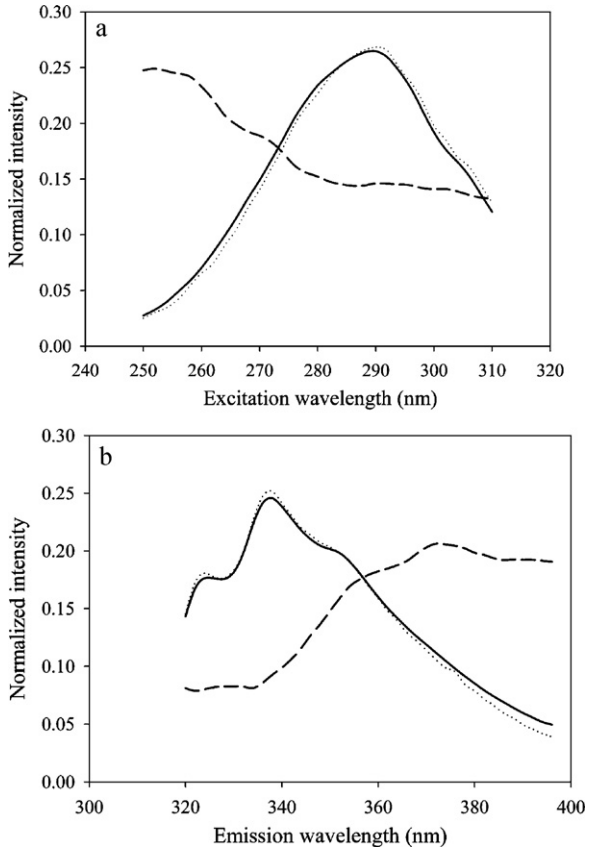

Fig. 5. Normalized excitation (a) and emission (b) profiles, which were resolved from EEM fluorescence of environmental samples by the APTLD method with two factors. Solid and medium-dash lines represent the spectral profiles of NAP and interference of environmental samples. The dotted line denotes the actual NAP.

Table 3
Results from APTLD analysis in the intra-day various matrices model of soil samples (*S*), sediment samples (*D*), wastewater samples (*W*), and river water samples (*R*), respectively.

Sample no.	Actual value of NAP ($ng\,mL^{-1}$)				Recovery (%)			
	S	*D*	*W*	*R*	*S*	*D*	*W*	*R*
P1	60	100	100	80	107.0	92.7	105.6	96.8
P2	80	130	130	100	104.1	101.2	104.1	100.7
P3	100	150	150	130	98.7	98.0	102.0	100.3
P4	130	170	170	150	96.8	105.2	102.7	99.8
P5	150	–	190	170	96.1	–	101.7	90.3
P6	170	–	200	190	106.5	–	102.4	94.9
Average recovery (%)					101.6 ± 4.3	99.3 ± 3.9	103.1 ± 1.2	97.1 ± 3.1
RMSEP ($ng\,mL^{-1}$)					6.39	6.88	4.95	9.48
REP (%)					5.56	5.00	3.16	6.69

Table 4
Results from APTLD analysis in the global model of soil samples (*S*), sediment samples (*D*), wastewater samples (*W*), and river water samples (*R*), respectively.

Sample no.	Actual value of NAP ($ng\,mL^{-1}$)				Recovery (%)			
	S	*D*	*W*	*R*	*S*	*D*	*W*	*R*
P1	60	100	100	80	100.2	88.3	113.7	108.3
P2	80	130	130	100	98.7	97.4	110.0	109.5
P3	100	150	150	130	94.1	94.5	107.3	106.9
P4	130	170	170	150	93.0	101.8	107.0	105.4
P5	150	–	190	170	92.6	–	105.9	94.9
P6	170	–	200	190	103.1	–	106.5	99.4
Average recovery (%)					97.0 ± 3.7	95.5 ± 4.1	108.4 ± 2.3	104.1 ± 4.6
RMSEP ($ng\,mL^{-1}$)					7.34	8.67	13.50	8.66
REP (%)					6.38	6.31	8.62	6.11

ronmental samples through a linear regression. The correlation coefficients of NAP obtained by using the APTLD algorithm with $N = 2$ was 0.9929. The concentrations of NAP in the environmental samples of various matrices are summarized in Table 4, together with the percentage of recovery. The average recoveries acquired from soil, river sediment, wastewater and river water samples were $(97.0 \pm 3.7)\%$, $(95.5 \pm 4.1)\%$, $(108.4 \pm 2.3)\%$ and $(104.1 \pm 4.6)\%$, respectively.

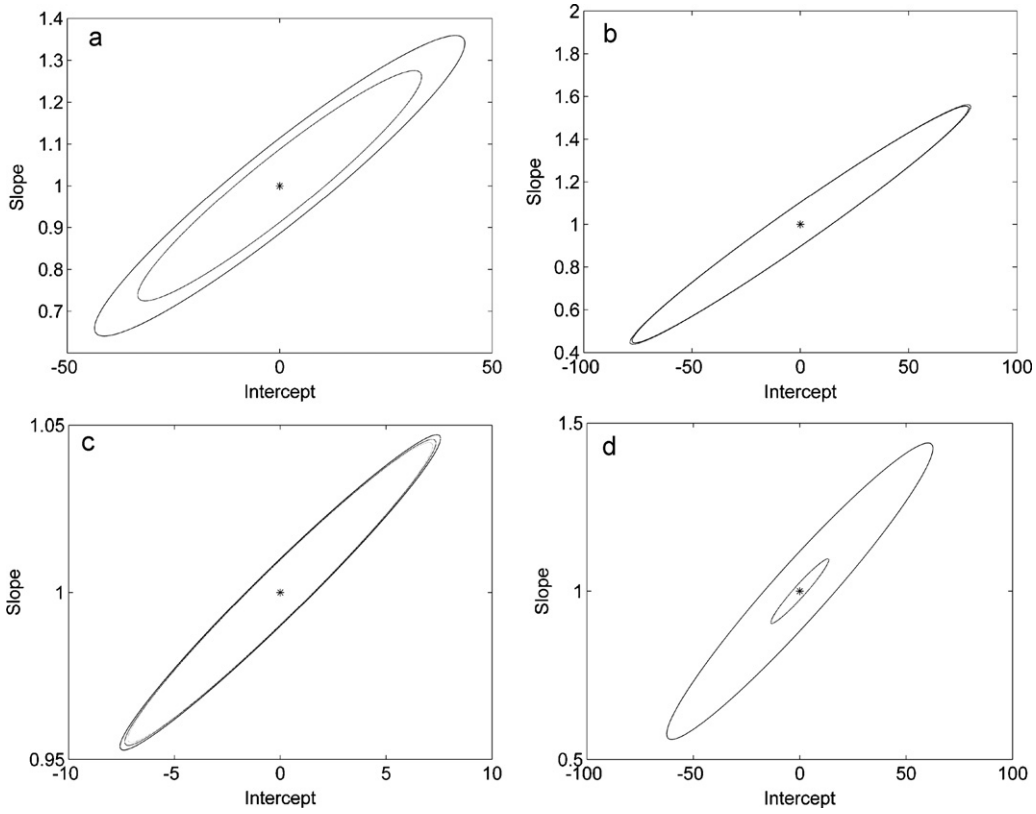

Fig. 6. EJCRs plots for NAP in environmental samples of various matrices: (a) soil samples, (b) river sediment samples, (c) wastewater samples and (d) river water samples. The asterisk (*) indicates the ideal points (0,1), long-dash, dotted and solid lines correspond to the EJCRs from the single matrix model, the intra-day various matrices model and the global model, respectively.

Single matrix model and intra-day various matrices model were very similar in behavior, which was also expected. From Tables 1, 3 and 4, we can see that there was no remarkable discrepancy between the results obtained by single matrix model and those provided by intra-day various matrices model. It proved that the second-order calibration methods have the ability to determine the analytes in various matrices simultaneously. The results in Table 4 are not so good as the results in Tables 1 and 3. Moreover, for the sake of a further investigation into the accuracy of the three types model based on the APTLD algorithm in environmental samples, an intra-laboratory testing of accuracy of analytical methods from recovery assays, i.e. linear-regression analysis of the actual *versus* the predicted concentrations was applied [33]. The calculated intercept and slope were compared with their theoretically expected values (0,1), based on the elliptical joint confidence region (EJCR) test. If the ellipses contain the values (0,1) for intercept and slope, respectively, showing the reference values and results do not present significant difference at the level of 95% confidence and the elliptic size denotes precision of the analytical method, smaller size corresponds to higher precision [34]. Fig. 6 gives the results of EJCRs for NAP in soil, river sediment, wastewater and river water samples with the APTLD algorithm in three types models, respectively. From the figure, it showed that the ellipses include the theoretically expected values of (0,1) labeled with a star (*), and the elliptic size corresponding to the global model is bigger than those related to the single matrix model and the intra-day various matrices model, indicating the accuracy of the used methodology. These results further proved that the three types of models based on the APTLD algorithm could allow for accurate determination of NAP in soil, sediment, wastewater and river water samples, and the single matrix model and the intra-day various matrices models are better than global model. Such a result may be ascribed to two reasons, in the global model, the data of different day were stacked together, the variability from day to day was existed [18]; on the other hand, the prediction quality may be affected by the ratio of size of calibration set and size of prediction set; for the same calibration set, the more prediction samples, the error may be bigger.

4. Conclusion

We developed a rapid, simple and selective method for the direct determination of napropamide (NAP) in the environmental samples of various matrices. It was based on the APTLD analysis of the excitation–emission matrix fluorescent spectra of NAP. Only with a simple pretreatment procedure, satisfactory results could be obtained for NAP in the environmental samples with various types of matrices, even in the presence of the interferences of environmental samples, fully exploiting "second-order advantage". Furthermore, the figures of merit, i.e. sensitivity, selectivity and limit of detection, as well as limit of quantification, were evaluated. Moreover, the single matrix model, the intra-day various matrices model and the global (inter-daily various matrices) model were investigated by the second-order calibration method based on the APTLD algorithm, which demonstrated the maintenance of the "second-order advantage" in simultaneous determinations of the analyte of interest in the environmental samples of various matrices. The calculated results revealed that such an approach can become a promising alternative for practical applications in environmental quality control to achieve the higher sensitivity and enhance the selectivity.

Acknowledgements

The authors gratefully acknowledge the National Natural Science Foundation of China (Grant No. 20775025) and the Program for Changjiang Scholars and Innovative Research Team in University (PCSIRT) for financial supports.

References

[1] K.S. Booksh, B.R. Kowalski, Anal. Chem. 66 (1994) 782A–791A.
[2] A.C. Olivieri, Anal. Chem. 80 (2008) 5713–5720.
[3] V. Gómez, M.P. Callao, Anal. Chim. Acta 627 (2008) 169–183.
[4] G.M. Escandar, N.M. Faber, H.C. Goicoechea, A.M. de la Peña, A.C. Olivieri, R.J. Poppi, Trends Anal. Chem. 26 (2007) 752–765.
[5] R.A. Harshman, UCLA Working Papers in Phonetics, vol. 16, 1970, pp. 1–84.
[6] J.D. Carroll, J.J. Chang, Psychmetrika 35 (1970) 283–319.
[7] E. Sánchez, B.R. Kowalski, Anal. Chem. 58 (1986) 496–499.
[8] R. Tauler, Chemometr. Intell. Lab. Syst. 30 (1995) 133–146.
[9] H.L. Wu, M. Shibukawa, K. Oguma, J. Chemometr. 12 (1998) 1–26.
[10] Z.P. Chen, H.L. Wu, J.H. Jiang, Y. Li, R.Q. Yu, Chemometr. Intell. Lab. Syst. 52 (2000) 75–86.
[11] A.L. Xia, H.L. Wu, D.M. Fang, Y.J. Ding, L.Q. Hu, R.Q. Yu, J. Chemometr. 19 (2005) 65–76.
[12] A.M. de la Peña, A.E. Mansilla, D.G. Gómez, A.C. Olivieri, H.C. Goicoechea, Anal. Chem. 75 (2003) 2640–2646.
[13] T. Madrakian, A. Afkhami, M. Mohammadnejad, Anal. Chim. Acta 645 (2009) 25–29.
[14] J.W.B. Braga, C.B.G. Bottoli, I.C.S.F. Jardim, H.C. Goicoechea, A.C. Olivieri, R.J. Poppi, J. Chromatogr. A 1148 (2007) 200–210.
[15] Y. Zhang, H.L. Wu, A.L. Xia, Q.J. Han, H. Cui, R.Q. Yu, Talanta 72 (2007) 926–931.
[16] M.J. Culzoni, R.Q. Aucelio, G.M. Escandar, Talanta 82 (2010) 325–332.
[17] J.F. Nie, H.L. Wu, X.M. Wang, Y. Zhang, S.H. Zhu, R.Q. Yu, Anal. Chim. Acta 628 (2008) 24–32.
[18] D. Giméneza, L. Sarabiab, M.C. Ortiz, Anal. Chim. Acta 544 (2005) 327–336.
[19] Á. Rinnan, J. Riu, R. Bro, J. Chemometr. 21 (2007) 76–86.
[20] P.K. Biswas, S.K. Pramanik, S.R. Mitra, A. Bhattacharyya, Bull. Environ. Contam. Toxicol. 79 (2007) 566–569.
[21] J.A. Murillo Pulgarín, L.F. García Bermejo, Anal. Chim. Acta 491 (2003) 37–45.
[22] J. Cui, R. Zhang, G.L. Wu, H.M. Zhu, H. Yang, Arch. Environ. Contam. Toxicol. 59 (2010) 100–108.
[23] W.L. Liu, Chin. J. Pestic. 45 (2006) 40–42.
[24] A. Lorber, Anal. Chem. 58 (1986) 1167–1172.
[25] A.C. Olivieri, N.M. Faber, J. Chemometr. 19 (2005) 583–592.
[26] A.C. Olivieri, Anal. Chem. 77 (2005) 4936–4946.
[27] A.C. Olivieri, N.M. Faber, Chemometr. Intell. Lab. Syst. 70 (2004) 75–82.
[28] K. Faber, B.R. Kowalski, Anal. Chem. 69 (1997) 1620–1626.
[29] S.H. Zhu, H.L. Wu, A.L. Xia, Q.J. Han, Y. Zhang, R.Q. Yu, Talanta 74 (2008) 1579–1585.
[30] Y.N. Li, H.L. Wu, J.F. Nie, S.F. Li, Y.J. Yu, S.R. Zhang, R.Q. Yu, Anal. Meth. 1 (2009) 115–122.
[31] Y.N. Li, H.L. Wu, X.D. Qing, Q. Li, S.F. Li, H.Y. Fu, Y.J. Yu, R.Q. Yu, Anal. Chim. Acta 678 (2010) 26–33.
[32] R. Bro, H.A.L. Kiers, J. Chemometr. 17 (2003) 274–286.
[33] A.G. González, M.A. Herrador, A.G. Asuero, Talanta 48 (1999) 729–736.
[34] J.A. Arancibia, G.M. Escandar, Talanta 60 (2003) 1113–1121.